

Biomimetic and mesoporous nano-hydroxyapatite for bone tissue application: a short review

Original

Biomimetic and mesoporous nano-hydroxyapatite for bone tissue application: a short review / Molino, Giulia; Palmieri, MARIA CHIARA; Montalbano, Giorgia; Fiorilli, SONIA LUCIA; VITALE BROVARONE, Chiara. - In: BIOMEDICAL MATERIALS. - ISSN 1748-6041. - 15:(2020). [10.1088/1748-605X/ab5f1a]

Availability:

This version is available at: 11583/2798735 since: 2020-02-28T09:05:38Z

Publisher:

IOP Publishing

Published

DOI:10.1088/1748-605X/ab5f1a

Terms of use:

This article is made available under terms and conditions as specified in the corresponding bibliographic description in the repository

Publisher copyright

(Article begins on next page)

TOPICAL REVIEW • **OPEN ACCESS**

Biomimetic and mesoporous nano-hydroxyapatite for bone tissue application: a short review

To cite this article: Giulia Molino *et al* 2020 *Biomed. Mater.* **15** 022001

View the [article online](#) for updates and enhancements.



IOP | ebooks™

Bringing you innovative digital publishing with leading voices to create your essential collection of books in STEM research.

Start exploring the **collection** - download the first chapter of every title for free.



TOPICAL REVIEW

OPEN ACCESS

RECEIVED
11 June 2019

REVISED
29 November 2019

ACCEPTED FOR PUBLICATION
5 December 2019

PUBLISHED
27 February 2020

Original content from this work may be used under the terms of the [Creative Commons Attribution 3.0 licence](#).

Any further distribution of this work must maintain attribution to the author(s) and the title of the work, journal citation and DOI.



Biomimetic and mesoporous nano-hydroxyapatite for bone tissue application: a short review

Giulia Molino¹, Maria Chiara Palmieri¹, Giorgia Montalbano, Sonia Fiorilli  and Chiara Vitale-Brovarone 

Department of Applied Science and Technology, Politecnico di Torino, Turin, Italy

¹ The first two authors equally contributed to the work.

E-mail: chiara.vitale@polito.it

Keywords: nano-hydroxyapatite, mesoporous, biomimetic, bone tissue, surfactants

Abstract

In the last decades, many research groups have experimented the synthesis of hydroxyapatite (HA) for bone tissue application obtaining products with different shapes and dimensions. This review aims to summarise and critically analyse the most used methods to prepare physiologic-like nano-HA, in the form of plates or rods, similar to the HA present in the human bones. Moreover, mesoporous HA has gained increasing interest in the biomedical field due its peculiar structural features, such as high surface area and accessible mesoporous volume, which is known to confer enhanced biological behaviour and the possibility to act as nanocarriers of functional agents for bone-related therapies. For this reason, more recent studies related to the synthesis of mesoporous HA, with physiological-like morphology, are also considered in this review. Since a wide class of surfactant molecules plays an essential role both in the shape and size control of HA crystals and in the formation of mesoporosity, a section devoted to the mechanisms of action of several surfactants is also provided.

1. Introduction

HA is the main inorganic constituent of human bone, representing around the 65%–70% of the bone mass. The organic phase, constituted mainly by type I collagen, counts instead around the 30 wt% of the bone mass, while the remaining part is constituted by water [1]. These materials are arranged in a very ordered structure allowing the bone to have peculiar properties. Type I collagen, indeed, is able to self-assemble into fibrils exhibiting a typical 67 nm banding pattern and forming 40 nm gaps between them. The HA crystals grow in these gaps in form of plates with average length of 50 nm, width of 25 nm and thickness of 2–3 nm and orienting their *c*-axis parallel to the long axis of the collagen fibrils [2]. Therefore, collagen has an important role in the spatial regulation of HA crystals, triggering their nucleation and modulating the mineralisation process. In fact, in the first stage of the mineralisation process the particles grow rapidly in two dimensions, being delimited by the collagen fibrils gap (primary mineralisation) [3]. In this phase, an intense ionic exchange between the core of the forming mineral particle and the surrounding aqueous biological fluids takes place. For this reason, HA crystals

present in the human bone are non-stoichiometric, with a Ca/P ratio of less than 1.67, and show different ion substitutions, where the most abundant one is represented by carbonate ion (CO_3^{2-}) in the amount of 3–8 wt% [4, 5]. The second stage of the mineralisation process, instead, is characterised by the increase of the mineral particle thickness and the reduction of the ionic exchange (secondary mineralisation). HA, however, remains a dynamic entity thanks to its large specific surface (around $100 \text{ m}^2 \text{ g}^{-1}$) that makes it metabolically active [6].

With the aim of mimicking the physiologic characteristics of HA, many studies have been conducted for the synthesis of nanometric HA with a grain size less than 100 nm in at least one direction. In addition, nanometric materials have unique surface properties that differ from those of conventional micro-sized materials and lead to a greater reactivity [7]. Nanosized HA, in fact, due to its peculiar surface properties (high surface area and increased roughness) exhibits enhanced resorbability and higher bioactivity, promoting better cell adhesion and cell-matrix interactions [8].

Therefore, the control of HA microstructure (morphology, stoichiometry, crystallinity and phase

purity) allows to modulate to some extent its mechanical and biological behaviour. For this reason, many efforts have been made to engineer HA crystals by developing new synthesis routes or modification of pre-existing methods in order to overcome their drawbacks [8], briefly described in the following. One of the synthesis routes largely adopted in the past due to its simplicity is the solid-state method, where HA precursors are first milled and then calcined. However, this method requires very high temperatures (around 1000 °C) and leads to powder with heterogeneous phase composition and irregular shapes [8]. Another common conventional synthesis method is HA chemical precipitation in an aqueous solution that involves the dropwise addition of a calcium solution into a phosphate one under stirring. The resultant solution is aged under atmospheric pressure and then is washed, filtered or centrifuged, dried and crushed into a powder. This method is simple but it presents several disadvantages, such as non-stoichiometric composition, low phase purity, poor crystallisation and non-uniform particle shapes [8, 9]. These aspects are normally associated with a significant reactivity in aqueous environments resulting in the uncontrolled agglomeration due to the formation of hydrogen bonds among HA particles [7, 8].

These two methods are not particularly suitable to produce HA for biomedical applications, such as drug delivery systems or as inorganic phase in hybrid devices for bone tissue engineering, where tailored morphological and chemical features are required in order to attain a controlled and reproducible biological effect. This essential requirement has shifted the research focus towards the investigation of novel synthesis methods able to produce powders with controlled phase composition, shape, size and crystallinity. Among them, three main synthesis methods have emerged as the most promising for the production of HA with controlled characteristics: the hydrothermal route, the microwave-assisted method and the emulsion-based method. In the hydrothermal process, the HA precursors are mixed in an aqueous environment and the aging step of the synthesis mixture is conducted inside an autoclave or a pressure vessel at high temperatures and elevated pressures. This process allows obtaining HA nanoparticles with relatively controlled stoichiometry, high crystallinity and rod-like shape [8, 9].

The microwave-assisted method is the fastest one to produce HA with high purity and controlled shape thanks to the uniform heating of the entire reaction volume. In this procedure, the aqueous solution containing the calcium and phosphate precursors is irradiated inside a microwave oven, usually employing a power higher than 500 W applied for a period not superior to 30 min. In contrast to the hydrothermal approach, where the material is externally heated through conduction, microwave irradiation involves *in situ* conversion of microwave energy into heat [8],

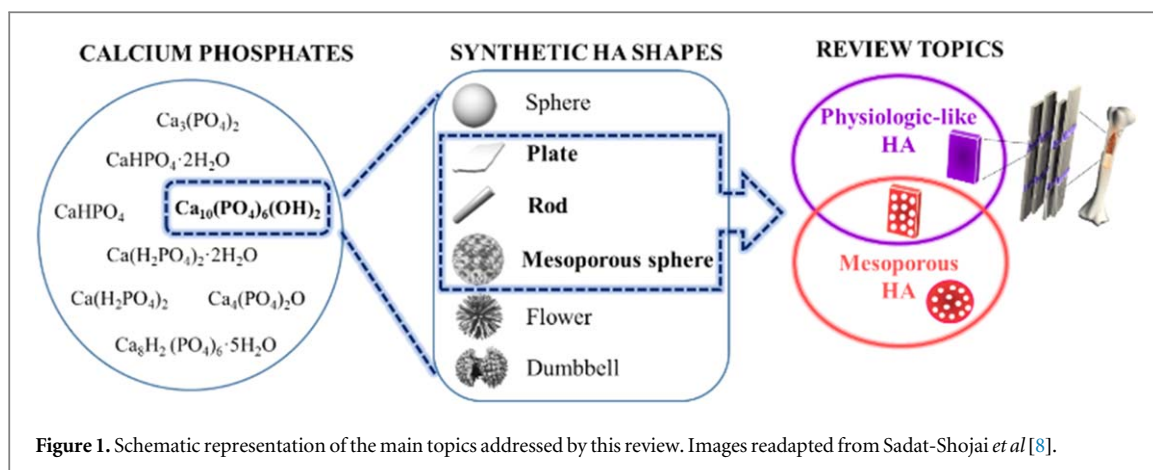
leading to a sizable increase of the reaction kinetics. As a result, the time requested for HA particle formation is reduced from several hours, required by the traditional synthesis, to few tens of minutes.

Concerning the emulsion method, the most common procedure for the synthesis of HA particles is based on a water-in-oil approach (W/O). In this process, the aqueous solution containing the HA precursors is dispersed dropwise in an oil phase containing a surface-active agent that, reducing the surface tension at the interface of the two liquids, allows the self-assembling of micelles. The formed micelles consequently provide a suitable and stable environment for the controlled nucleation of HA particles, without the requirement of high-temperature conditions.

With the aim to further enhance the control over the HA nanostructure, the above-mentioned synthesis methods have been often combined with the use of surfactants. In fact, when introduced in a solution of calcium and phosphate precursors over their critical micelle concentration (CMC), surfactants are able to self-assemble in micelles with a specific shape and act as templates for the controlled nucleation and growth of HA crystals [4]. In particular, their chemical features, especially the molecular weight and the ratio between hydrophobic tail and hydrophilic head, strongly influences the final morphology and size of HA particles [8, 9]. Moreover, HA particles synthesized without the use of surfactants showed a higher tendency to aggregate [10]. On the other hand, the addition of controlled amount of surfactants in HA solutions have been successfully used to introduce nanoporosity in the HA particles, particularly in the mesoporous range (2–50 nm). Due to the multifunctional role exerted by surfactants in the HA synthesis, a specific part of this review (section 2) has been devoted to the description of their mechanism of action.

In the literature, previous reviews have already reported and discussed the large number of synthesis routes to obtain HA and other calcium phosphates (CaPs) with controlled shape and size [7, 9]. In particular, in the review of Lin *et al* [9], several synthesis methods to obtain calcium phosphate crystals with different structures (spheres, rods, plates, whiskers, flowers or dumbbells) are accurately described. However, some of these shapes are quite dissimilar from that shown by physiologic HA crystals, making them not appropriate for applications where biomimicry is sought. Other reviews were focused also on the potential biomedical applications of CaPs [11–13]. For instance, Uskoković Vuk and Uskoković Dragan [11] dedicated their review on the application of CaPs as drug delivery systems for diagnosis and therapy, while Dorozhkin and Epple [13] reviewed the application of CaPs in the orthopaedic field.

With a specific focus on HA, Sadat-Shojai *et al* [8] accurately described the synthesis processes to obtain



nanosized crystals with various structures, spanning from the physiologic-like (plate or rods) to the more complex ones (whiskers, flowers or dumbbells). In addition, several authors have reviewed the application of HA in the biomedical field as bone substitutes [5, 14], drug delivery systems [4] or the combination of both [15].

With the present review, the authors aim to focus on the methods used to synthesize biomimetic HA in the form of nanometric plates or rods. Our objective is to guide the readers towards the selection of the most suitable methods to produce HA for biomedical applications, in particular for bone tissue regeneration and biomimetic systems. The second goal of this review is a critical resume of the proposed approaches across the literature to produce mesoporous HA with improved biological performances thanks to the significant increase of the exposed surface area. To the best of the authors' knowledge, this review is the first one specifically focussing on biomimetic and mesoporous HA as well as on synthesis routes able to combine these two aspects.

For the sake of clarity, the main topics covered in this review are schematically depicted in figure 1.

2. Role of surfactants in hydroxyapatite synthesis: mechanism of action

According to the literature data, three types of surfactants have been generally adopted for the synthesis of HA: cationic, anionic and non-ionic. The most used cationic surfactant is cetyltrimethylammonium bromide (CTAB) which consists of a positively charged hydrophilic head and a hydrophobic tail. When dissolved in an aqueous medium above its CMC (0.001 M), CTAB can form rod-like micelles exposing positively charged groups (CTA^+), able to interact electrostatically with the phosphate ions. Furthermore, CTA^+ and phosphate ions share the same tetrahedral structure which makes them stereochemically compatible to interact with each other, acting as a very effective nucleation site for HA when the calcium precursors are added in the solution [16, 17].

A mechanism similar to that performed by CTAB, based on charge and structure complementarity, was proposed by Kolodziejczak *et al* [18] for sodium dodecyl sulphate (SDS), used as anionic surfactant for the synthesis of HA nanorods. The sulphate groups of SDS are indeed able to interact electrostatically with calcium ions and, resulting in numerous calcium-rich domains. When phosphate sources are added to the synthesis mixture, the rapid formation of ordered HA particles occurs.

Sodium bis(2-ethylhexyl) sulfosuccinate (AOT) is another sulphur-containing surfactant that is widely used in W/O emulsions since it forms stable reverse micelles over a wide range of water/surfactant mole ratios, by exposing its sulphur-containing head towards the aqueous environment and its hydrophobic tail toward the oil phase. Thanks to its sulfonate group, AOT can also act as an anionic surfactant suitable for the synthesis of rod-like nano-HA [19]. In fact, by exploiting the strong affinity of sulfonate ions towards Ca^{2+} , the latter can be strongly bonded to the AOT micelle surface at W/O interface. After the addition of the phosphate precursor to the microemulsion solution, PO_4^{3-} ions bind to the calcium ions, thus leading to the nucleation of HA at the AOT micelle surface and the successive crystal growth along a preferential direction deriving by the AOT micellar structure [20].

Compared to the previous reported anionic surfactants, ethylene diamine tetracetic acid (EDTA) exploits a different mechanism to direct the growth of HA. In fact, EDTA acts as a hexadentate ligand by packing itself around the free Ca^{2+} ions, controlling subsequently the nucleation and growth of HA nanocrystals. As a result of this complexation, the quantity of free Ca^{2+} ions decreases leading to the formation of smaller HA nuclei. The HA formation rate and the crystallite growth is determined by the stability of these Ca-EDTA complexes that in turn depends on the pH medium. For example, at pH at least equal to 9, sufficient free Ca^{2+} ions are released from Ca-EDTA complexes and can be incorporated into the crystal lattice sites contributing to the crystallite growth. At

variance at pH values below 9, the nanocrystal formation does not occur, most likely due to the low stability of Ca-EDTA complexes [21].

A similar mechanism of action can be obtained by adding sodium tripolyphosphate (STPP) in the calcium solution: STPP acts as an effective calcium chelating agent controlling its availability in the solution and, consequently, modulating the morphology of HA crystals toward plate-like shapes [22].

Among the non-ionic surfactants employed in the synthesis of HA Triton X-100, polyethylene glycol (PEG) and Pluronic F127 are worth mentioning. According to Iyyappan *et al* [23], Triton X-100 is able to interact with the calcium ions thanks to its polyoxyethylene (EO) groups through the creation of ion-dipole interactions and thereby forming a hydrophobic open ring complex. This complex can create Van der Waals interactions with the -OH groups at the surface of the growing HA crystals, facilitating the growth of nanoparticles along a preferential direction [23]. The ability of Triton X-100 to direct the alignment of small HA crystallites was also confirmed by Zhang *et al* [24] that proposed a coordination mechanism between EO segments in Triton X-100 and Ca^{2+} leading to the precipitation of HA at the hydrophilic surface of the surfactant micelles and the consequent formation of nanorods. In another work, Iyyappan *et al* [25] suggested that the open-ring complexes formed by Triton X-100 can also hinder the agglomeration of HA particles. Due to the formation of these complexes, in fact, the transfer rate of calcium ions from the open ring complex to the growing HA crystal is reduced and, therefore, the formation of nanosized HA crystals takes place in a controlled manner.

Azzaoui *et al* [26] reported a similar mechanism based on the controlled release of calcium ions by PEG-1000 (MW 1000), which is supposed to chelate Ca^{2+} ions reducing the extent of their interactions with phosphate ions and consequently allowing the HA nucleation with a more controlled kinetics.

Concerning Pluronic F127, Zhao and Ma [27] investigated the effect of two different concentrations of this surfactant obtaining HA with two different shapes: spherical particles were found for higher concentration (0.1 g ml^{-1}) and rod-like for lower concentration (0.03 g ml^{-1}). They supposed that Pluronic F127, through the engagement of hydrogen bonds with the calcium precursor (calcium D-pantothenate monohydrate), provides multiple sites for nucleation of shape-controlled HA crystals.

Figure 2 summarises the chemical structure of the above-mentioned surfactants and chelating agents used for HA synthesis and their general mechanism of action. Figure 3(A) schematically reports the mechanism of action of a charged surfactant exploiting the electrostatic interaction with the phosphate or calcium ions to direct the HA growth in a preferential direction. The same figure illustrates also the behaviour of a

surfactant acting as a calcium-chelating agent (figure 3(B)).

3. Physiological-like shaped hydroxyapatite

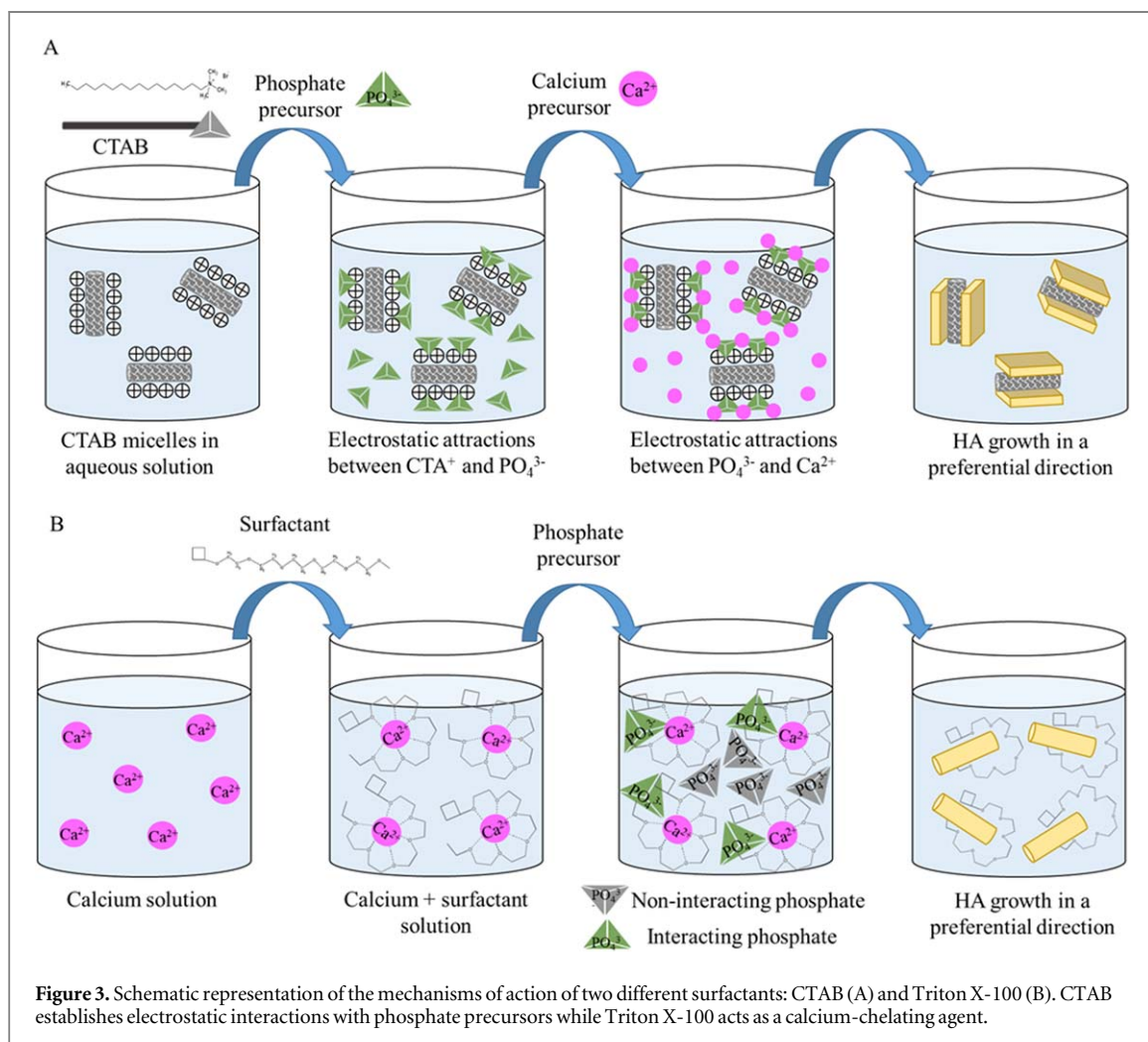
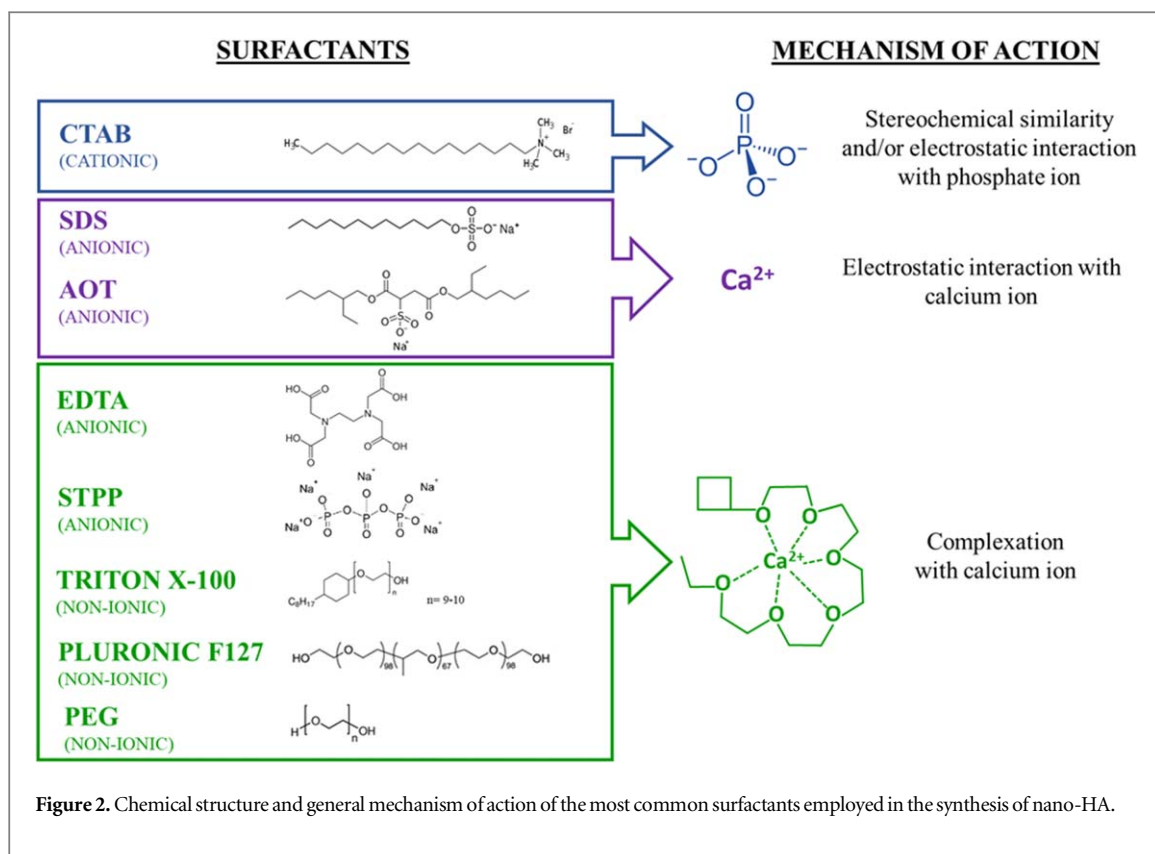
3.1. Plate-like HA

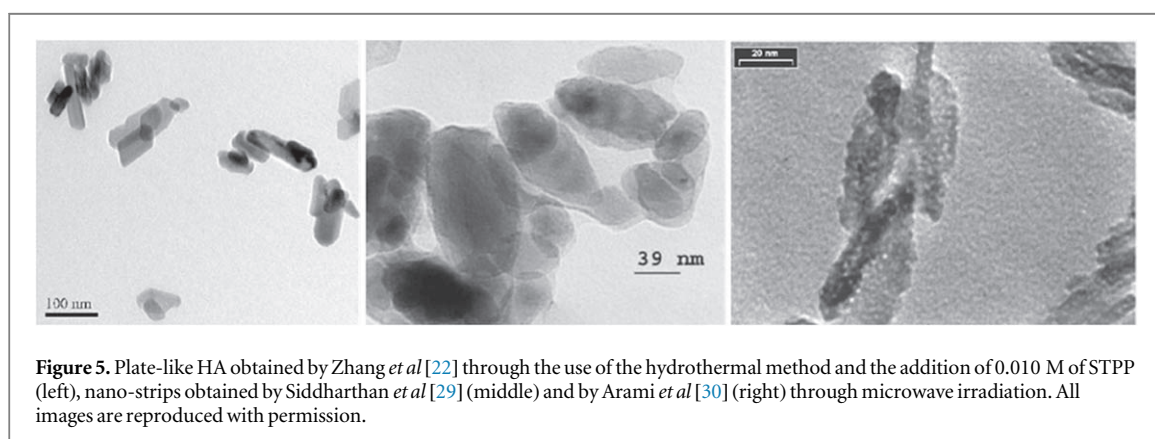
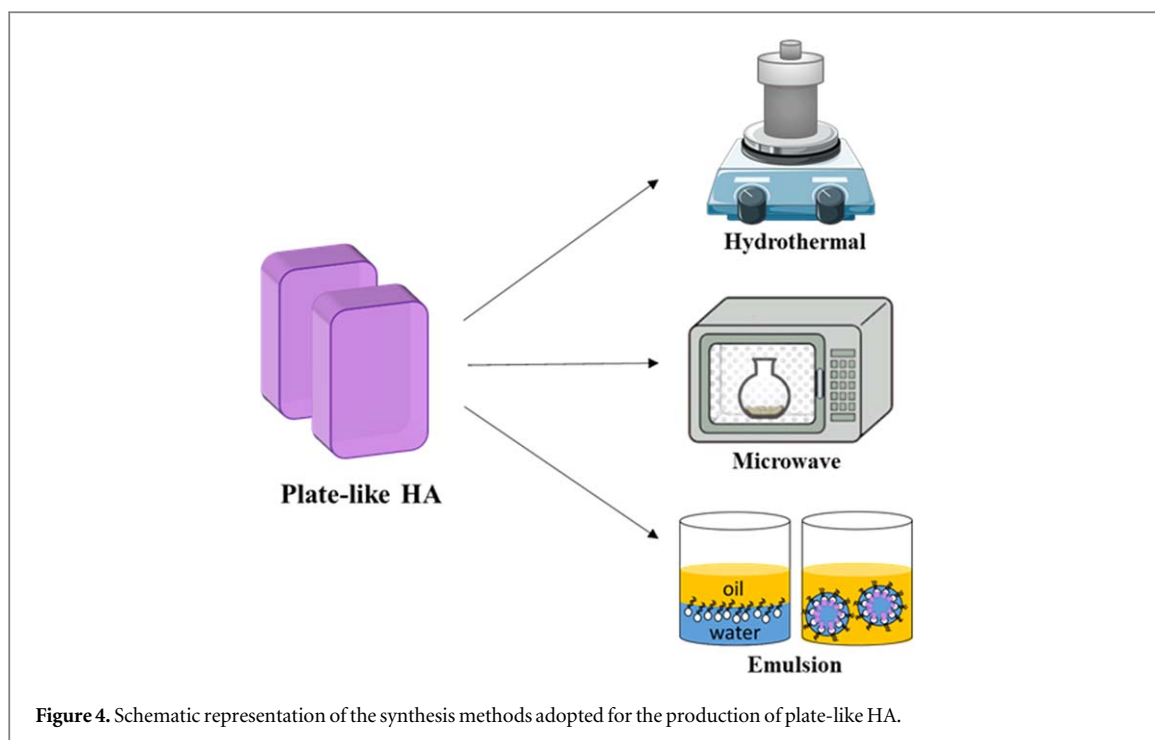
The synthesis of plate-like HA has been investigated by various research groups with the aim of mimicking the natural inorganic phase of bone for their use in different bone tissue engineering applications. However, the formation of a physiological shape is hindered by the strong HA tendency to form spherical nanoparticles in aqueous environments [7]. For this reason, non-conventional synthesis methods have been investigated in order to obtain plate-like nanoparticles, i.e. hydrothermal, emulsion and microwave irradiation techniques, as represented in figure 4.

The hydrothermal synthesis is one of the most common methods for the preparation of nano-sized HA, although usually with poor control over its morphology. For this reason, this technique has been frequently combined with the use of various surfactants in order to regulate HA crystal growth and, consequently, to modify its morphology.

Among the research groups that have successfully obtained plate-like HA, it is worth mentioning Nagata *et al* [28] who reported the preparation of plate-like HA particles by means of an hydrothermal treatment with the aid of ethylamine which led to a wide a-plane growth. In this synthesis plate-like crystals of about 50–300 nm in size were obtained by using CaCO_3 and $\text{CaHPO}_4 \cdot 2\text{H}_2\text{O}$ as calcium and phosphate sources respectively and by treating the synthesis mixture, containing at least 5 wt% of ethylamine, in a hydrothermal reactor at 180 °C for 5 h.

Zhang *et al* [22] successfully synthesized plate-like nanoparticles of HA with different aspect ratios (length/width) by means of the hydrothermal method adding STPP, as chelating agent, in different concentrations. Calcium nitrate and disodium hydrogen phosphate were used as calcium and phosphorous sources respectively and ammonium hydroxide was employed to adjust the pH value (between 8 and 10). The resulting mixture was hydrothermally treated at 160 °C for 4–12 h. The authors noticed that the aspect ratios decreased with increasing concentrations of STPP, evidencing a significant influence of the latter on the final morphology of HA crystals: in particular, by increasing STPP concentration, the diameter of HA widened while the length decreased. At STPP concentration equal to 0.010 M, the HA crystals were plate-like (figure 5 left) with a mean aspect ratio close to 2, indicating a structure with a length double than the width, similarly to physiologic HA. Therefore, the authors concluded that STPP surfactant, mainly acting as crystal growth directing agent, is able to regulate the growth of HA particles in the form of plates.





Another technique successfully employed in the synthesis of plate-like HA is the emulsion method. As previously described, through this method a stable suspension of two immiscible liquids, such as water and oil, is formed and the emulsion droplets act as reactors for the nucleation and growth of HA crystals. The addition of surfactants stabilizes the emulsion by reducing the surface tension of the immiscible liquids and forming nanosized liquid droplets, that consequently lead to nanometric HA particles formation [31]. Through this method, Sato *et al* [19] obtained crystals with an elongated plate-like shape using AOT and cyclohexane (C_6H_{12}) as the oil phase. A solution containing phosphorus (KH_2PO_4) and calcium ($Ca(OH)_2$) precursors constituted, instead, the aqueous phase. The authors observed that the presence of HA precursors in a supersaturated concentration was a key parameter to modulate the crystal growth. In fact, by testing two different $[AOT]/[Ca^{2+}]$ molar ratios, they observed that in higher supersaturation

conditions ($[AOT]/[Ca^{2+}] = 540$ wt%) a more intense growth of HA crystal nuclei was fostered. The obtained plate-like crystals had, in fact, bigger dimensions ranging between 50 nm and 200 nm in length and of about 10 nm in thickness. In lower supersaturation conditions ($[AOT]/[Ca^{2+}] = 21.6$ wt%), instead, the obtained crystals were smaller with round shape, due to the lower HA precursors amount available for crystal growth.

In addition to the previous reported methods, microwave irradiation is reported to be an efficient route to obtain high purity HA providing a rapid, facile and convenient synthesis procedure. Siddharthan *et al* [29] found out that HA particles with different shape and size could be prepared by selecting a suitable microwave power. In fact, they obtained needle-shaped particles (lengths of 39–56 nm and widths of 12–14 nm) at 175 W, acicular (lengths of 10–16 nm and widths of 10–12 nm) at 525 W and platelet (lengths of 32–42 nm and widths of 12–25 nm) at

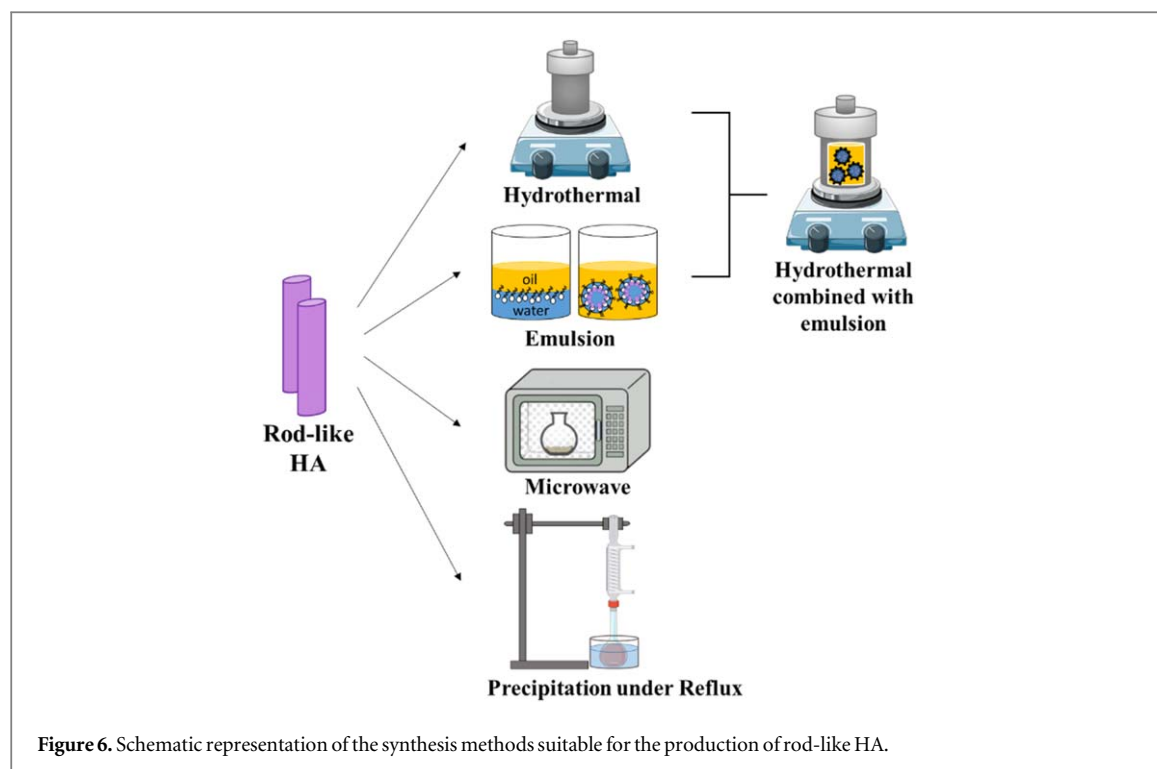


Figure 6. Schematic representation of the synthesis methods suitable for the production of rod-like HA.

660 W (the latter are visible in figure 5 middle). Similarly, through the microwave irradiation (2.45 GHz and 900 W) for 5 min to a solution containing Na_2HPO_4 and $\text{Ca}(\text{NO}_3)_2 \cdot 4\text{H}_2\text{O}$ precursors and CTAB, Arami *et al* [30] synthesized HA nano-strips with an average width and length of about 10 nm and 55 nm, respectively (figure 5 right)

3.2. Rod-like HA

Many research studies have been dedicated to the synthesis of rod-like HA despite their inferior biomimicry if compared to nanoplates. Rod-like HA has been obtained mainly through hydrothermal method, emulsion synthesis, microwave irradiation and precipitation method in reflux condition (as schematically represented in figure 6), all assisted by the use of surfactants.

Concerning the HA synthesis in hydrothermal conditions, many works have focused on the use of CTAB as directing agent thanks to its ability to act as nucleating sites for PO_4^{3-} and Ca^{2+} ions, as described in section 2. In particular, Wang *et al* [32] studied the influence of the autoclaving temperature and the pH solution on the morphology of HA particles, using CaCl_2 and H_3PO_4 as HA precursors in presence of CTAB. They observed that the efficacy of CTAB to modify HA morphology was higher when the solution was maintained at mild basic conditions. More in detail, nearly round shaped particles were obtained at pH equal to 13, while at pH equal to 9 the morphology changed into rod-like (figure 7(b)). This behaviour was explained by the authors considering the different interaction between PO_4^{3-} ions and CTAB in response to a change of pH conditions. In fact, at higher pH the

crystallization of HA crystals in form of nanorods is disturbed by the increased concentration of hydroxyl ions (OH^-) in the aqueous solution that repulse the PO_4^{3-} and, consequently, hamper their interaction with the positively charged heads of CTAB. On the contrary, when the pH is lower, fewer OH^- ions are available in solution and, consequently, the rod-like structure is favoured. Moreover, the authors observed an increase in the average diameter and in the length of the synthesized crystals with the increase of the temperature from 90 °C to 150 °C, always maintaining a treatment duration of 20 h.

These results were further confirmed by the same authors in a more recent work [33], where they synthesized rod-like HA nanoparticles with uniform morphologies and controllable size by low-temperature hydrothermal methods in the presence of CTAB, but changing the phosphate precursor (K_2HPO_4 instead of H_3PO_4). They observed a modification of HA morphology due to the variation of the autoclave temperature between 60 °C and 150 °C and of the treatment duration from 12 h to 24 h. In particular, they noticed that with the temperature increase, the HA crystals became longer and thinner leading to a consequent increase in their aspect ratio. In fact, at 120 °C the crystal length and diameter were equal to 60 nm and 20 nm respectively, while for the samples obtained at 150 °C they were around 150 nm and 15 nm, leading to an aspect ratio of 10 (figures 7(c), (d)). In addition, they did not observe a significant variation of particle size and morphology with the increase of the reaction time and pure HA was always obtained. Therefore, they concluded that the reaction temperature had a stronger influence in controlling

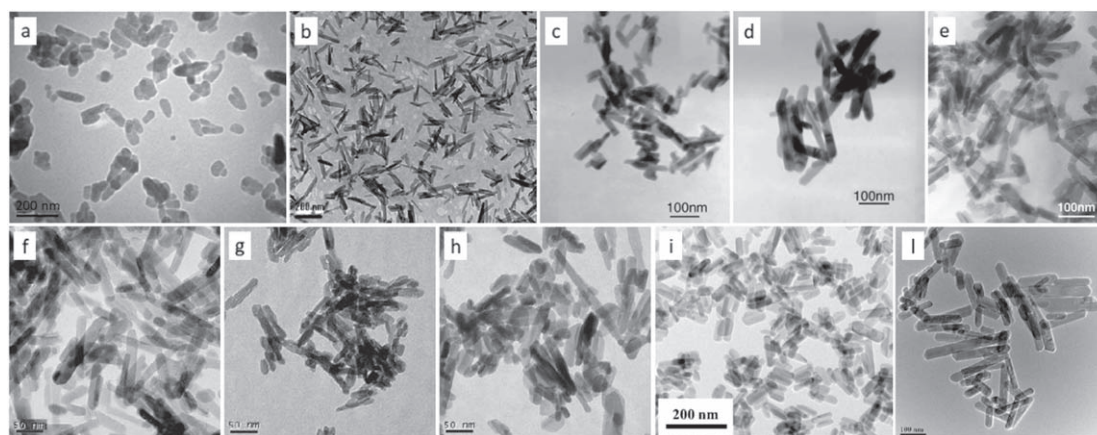


Figure 7. Rod-like HA particles obtained by different authors: (a) Iyyappan *et al* [25], (b) Wang *et al* [32], (c)–(d) Wang *et al* [33], through hydrothermal treatment at 120 °C for 24 h and at 150 °C for 20 h, (e) Yan *et al* [34], (f)–(h) Wang *et al* [35], with PEG, trisodium citrate and Tween 20, (i) Xin *et al* [36] and (l) Lin *et al* [37]. All images are reproduced with permission.

the crystal morphology and size, whereas the hydrothermal treatment duration seems to play a more negligible role.

In contrast to what stated by Wang *et al*, Yan *et al* collaborators [34] investigated more thoroughly the effect of the hydrothermal treatment duration on the shape of the final HA particles. In this contribution the authors tested two different solutions both with $\text{Ca}(\text{NO}_3)_2$ and Na_3PO_4 as HA precursors, but one containing CTAB and the other SDS, and inserting them in a Teflon-lined autoclave at 150 °C. In both cases, they obtained nanorods with length of 150 nm and diameter of 10 nm (as visible in figure 7(e)) if the reaction time was longer than 10 h. In particular, with shorter hydrothermal treatments (2 and 5 h), a mixture of fibres, rod and aggregates were obtained, while with treatment durations of 10 and 16 h the final product was composed exclusively of uniform nanorods.

Hydrothermal synthesis of rod-like HA has been also reported in the literature by using other anionic surfactants. For example, Xin *et al* [36] investigated the use of EDTA as capping agent, testing different pHs and autoclaving temperatures. They synthesized HA nanorods in the range from 50 to 200 nm in length, obtaining the most physiologic-like shape at pH 12 and with a vessel temperature of 180 °C, as shown in figure 7(i). The authors noticed that the precipitates from the alkaline solution were always composed of pure HA crystals, irrespective of the employed solution temperature. On the other hand, in the presence of an acidic solution, the hydrothermal temperature had great effects on the crystal structure of the precipitates. In fact, the transformation from DCPD (dicalcium phosphate dehydrate) to DCPA (dicalcium phosphate anhydrous) and from DCPA to HA occurred at specific temperatures. In the work of Xue *et al* [38], EDTA has been combined with CTAB, for the synthesis of HA through hydrothermal method (24 h at 180 °C) obtaining nanorods with lengths of 60–90 nm and widths of 10–20 nm.

Rod-like powders were also produced in the presence of organic agents, such as PEG (MW 600), Tween-20 and trisodium citrate (as visible in figures 7(f)–(h)), under alkaline conditions (pH = 10) and at different hydrothermal temperatures. For example, PEG-600 showed to be beneficial for the formation of HA nanorods with a larger aspect ratio at high synthesis temperature, as compared to Tween-20 and trisodium citrate, due to the increased flexibility of PEG molecules due to temperature rise. When Tween-20 was used as a surfactant, shorter and thicker HA nanorods were instead obtained, using an autoclaving temperature of 100 °C or 200 °C. This behaviour was attributed to the steric effect of the dendriform structure of Tween-20 and to its strong coordination action on the surfaces of the resulting HA nanorods. Finally, nanorods with the smallest sizes in both diameter and length were obtained with trisodium citrate, thanks to the strong interactions between the carboxyl groups of citrate anion and the surface of HA nanocrystallite. Moreover, as observed for CTAB, a higher autoclaving temperature favours the growth of HA crystals with rod shape also in the presence of these organic agents [35].

To summarize briefly, an abundance of data regarding the HA hydrothermal synthesis has been published, leading to some discrepancies regarding the optimal experimental conditions leading to rod-like morphologies. However, as a general consideration, all reported studies share some common features in order to produce nanorods: presence of an alkaline medium, autoclaving treatment at temperature above 100 °C and duration of about 20 h. Higher hydrothermal temperatures and longer treatments lead to the production of HA with high crystallinity and large crystal size.

Emulsion-based methods were also found to be successful in synthesizing nanorods with controlled size and shape. Sun *et al* [39] obtained rod-like structures with a shape of 8–15 nm in diameter and

25–50 nm in length by combining a series of surfactants (Triton X-100 and CTAB) and co-surfactants (*n*-butanol and *n*-hexanol) and by using cyclohexane as the oil phase. The authors adopted both non-ionic and ionic surfactants in order to have a double stabilization function at the interfacial film, resulting in a better control on the particle size and growth.

In order to obtain mono-dispersed rod-like particles with narrow size distribution and high crystallinity, Lin *et al* [37] combined the emulsion method with the hydrothermal treatment. They heated in an autoclave at 180 °C for 18 h a W/O microemulsion containing CTAB as surfactant agent, *n*-pentanol as cosurfactant, *n*-hexane as the oil phase and HA precursor solution as the water phase. In this way, they successfully synthesized stoichiometric single-crystal HA nanorods with a diameter of 25–40 nm and a length of 55–350 nm (figure 7(l)). The high homogeneity in size and shape was attributed to the W/O nanometric micelles and to the template agent action, while the high crystallization was due to the hydrothermal treatment.

Other authors synthesized monodispersed single-crystal HA particles through a simple, economic, repeatable and rapid microwave irradiation method. For example, Liu *et al* [40] reported the synthesis of HA through the microwave method in the presence of EDTA, obtaining different shapes by varying the pH. In particular, they obtained HA nanorods at pH value equal to 9 and a microwave treatment of 30 min at 700 W. Similarly, Lak *et al* [41] produced nanorods with nearly uniform diameters and lengths around 25 and 100 nm, respectively. More in detail, they placed a solution containing Na₂HPO₄ and Ca(NO₃)₂·4H₂O as HA precursors and EDTA in a microwave irradiation chamber (2.45 GHz, 900 W) in continuous heating mode for 150 s. More recently, Kalita *et al* [21] synthesized rod-shaped HA (around 5 nm in diameter and 15 nm in length) starting from the same reagents but applying the microwave radiation with a power of 600 W and a working cycle of 3 min on and 5 min off for a total period of 19 min.

Several works in the literature focus on the synthesis of rod-like HA through the precipitation under reflux of aqueous solutions containing a surfactant agent. In this condition, the vapours generated by heating the solutions are cooled by means of a reflux condenser, falling back in the solution, allowing to keep more constant the surfactant concentration throughout the reaction. Iyyappan *et al* [25], in fact, obtained rod-like HA particles between 35 and 72 nm in length and 16 and 26 nm in diameter (figure 7(a)) by refluxing for an hour a solution of Ca(NO₃)₂, (NH₄)₂HPO₄ and Triton X-100 under alkaline conditions (pH equal to 10.4). In a more recent work, Shiba *et al* [16] refluxed for 24 h at 40 °C a solution containing K₂HPO₄·3H₂O and CaCl₂ as HA precursors combined with CTAB. In particular, they found that, using a molar ratio of CTAB:PO₄³⁻ equal to 2:1,

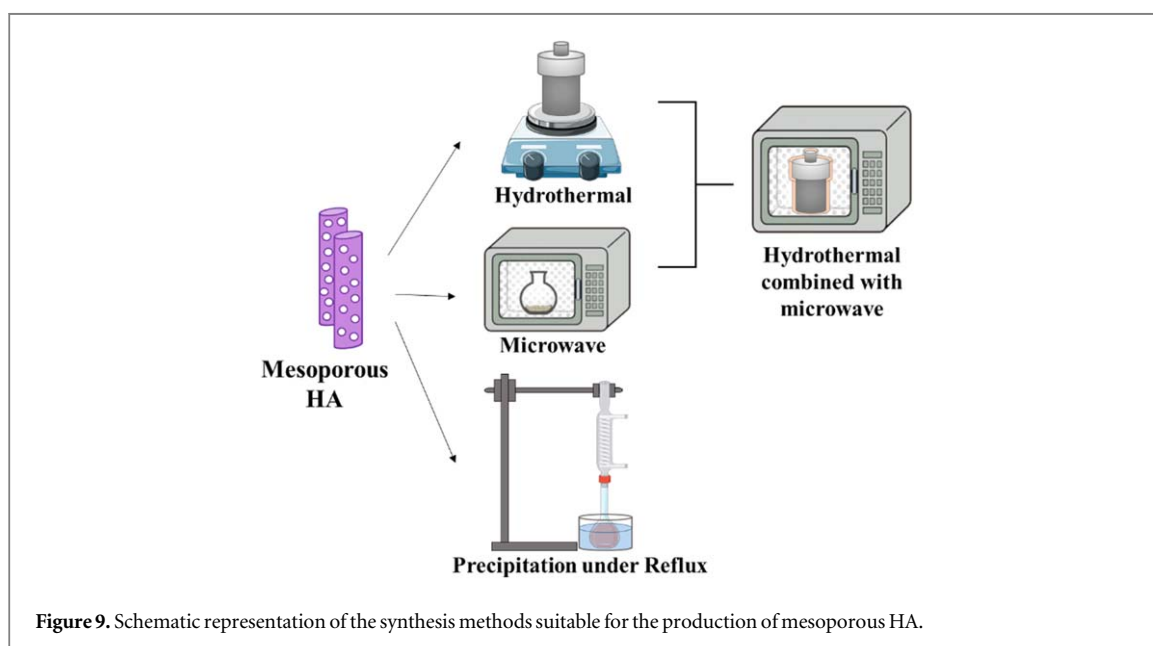
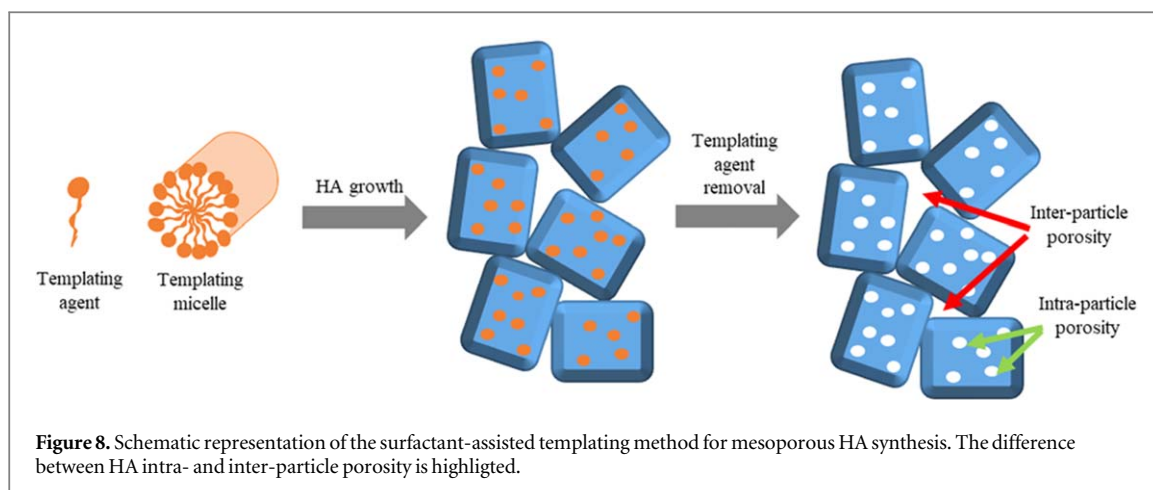
well-dispersed and uniform nanorods with a diameter of approximately 20 nm and a length of 50 nm were obtained.

On the other hand, some groups reported the synthesis of rod-like HA particles by simple wet chemical process combined with a surfactant agent. Wang *et al* [42] synthesized nanoscale rods by stirring a solution containing Ca(NO₃)₂, (NH₄)₂HPO₄ and ethanolamine with a pH of 10 for 1.5 h at 60 °C and then by ageing it for 24 h at room temperature. Similarly, Khalid *et al* [43] used the same calcium and phosphate precursors, but in association with CTAB, obtaining rod-like morphology. In particular, they stirred an alkaline solution (pH = 10) at 80 °C for 2 h and then they left it aging for 24 h at room temperature and in air. However, this type of synthesis is usually associated with a lack of control on the shape, the size and the crystallinity of the final product. In fact, Loo *et al* [44] found significant differences in the properties of HA particles synthesized using chemical precipitation or hydrothermal treatment. In the first case, they obtained rod-like particles with irregular shape and poor surface morphology, while the hydrothermal treatment allowed producing fine-grained and highly pure single crystals with more controlled morphology and narrow size distribution, reducing the particle agglomeration. Moreover, the hydrothermally produced HA showed a Ca/P molar ratio closer to the stoichiometric one [45].

4. Mesoporous HA

According to the IUPAC nomenclature [46], materials showing nanopores in the range from 2 to 50 nm are defined as mesoporous. Due to their peculiar textural features, i.e. high specific surface area and high pore volume, they have attracted the interest of the research community for a wide range of applications. Mesoporosity can result from the aggregation of primary nanoparticles or nanorods, leading to inter-particle voids, or from an intra-particles porosity generated through several methods mostly based on the use of porogen agents, among which the surfactant-assisted templating method is the most commonly adopted. Specifically, this method is based on the cooperative self-assembling of inorganic precursors around the surfactant micelles acting as templating agent, which upon calcination gives rise to the intra-particle mesoporosity.

Since this uniform and accessible intra-particle mesoporosity can be successfully exploited in the biomedical field, such as for drug storage and release and for bone tissue applications [47], several authors tried to apply the surfactant-assisted templating approach to the synthesis of mesoporous HA. Nevertheless, the most of the literature works report a prevalence of disorganized intra-particle pores, probably due to the high crystallisation rate of HA in aqueous solution that leads to the fast and consequently random growth of



HA grains around the templating micelles [17]. This high reactivity of HA precursors in aqueous environment is also accounted for the formation of aggregates, where particles are randomly organised and separated by voids at nanometric scale, as schematically represented in figure 8. These inter-particle voids are hardly distinguished from the intra-particle pores through adsorption-desorption measurements, due to their similar size and the wide-ranging distribution, ranging from few nanometres to several tens of nanometres. Since the templating agents usually produce mesopores whose size does not exceed 10–12 nm [48, 49], the contributions at higher pore size values are most likely due to the inter-particle contribution. TEM analyses are usually performed to discern the different contributions to the overall porosity evidenced by adsorption analysis, allowing the direct visualisation of the intra-particle porosity.

In this review, we refer to the different literature contributions concerning the production of mesoporous HA with physiologic-like shape, subdividing the works according to the employed templating agents.

In general, mesoporous HA is produced through the hydrothermal technique, the microwave irradiation method (or a combination of both) and the precipitation under reflux conditions, as schematically represented in figure 9.

Different authors successfully synthesized mesoporous HA using the hydrothermal treatment in combination with CTAB. For example, Li *et al* [50] produced mesoporous HA testing different autoclaving temperatures ranging from 40 °C to 160 °C and several calcination temperatures (550 °C, 700 °C, 800 °C and 1000 °C). They observed an increase of crystallinity and the formation of rod-like structures with the increase of the reaction temperature (figure 10(b)), while the nanopore size was found to decrease from about 5 nm at 40 °C to 2 nm at 160 °C, probably due to the higher crystallinity of the structure and the consequent tighter packing of atoms. At variance, pore size showed to be independent on both calcination temperature and CTAB/ PO_4^{3-} molar ratio: a finding in contrast to the most part of literature works that stated a key role of surfactant concentration in the

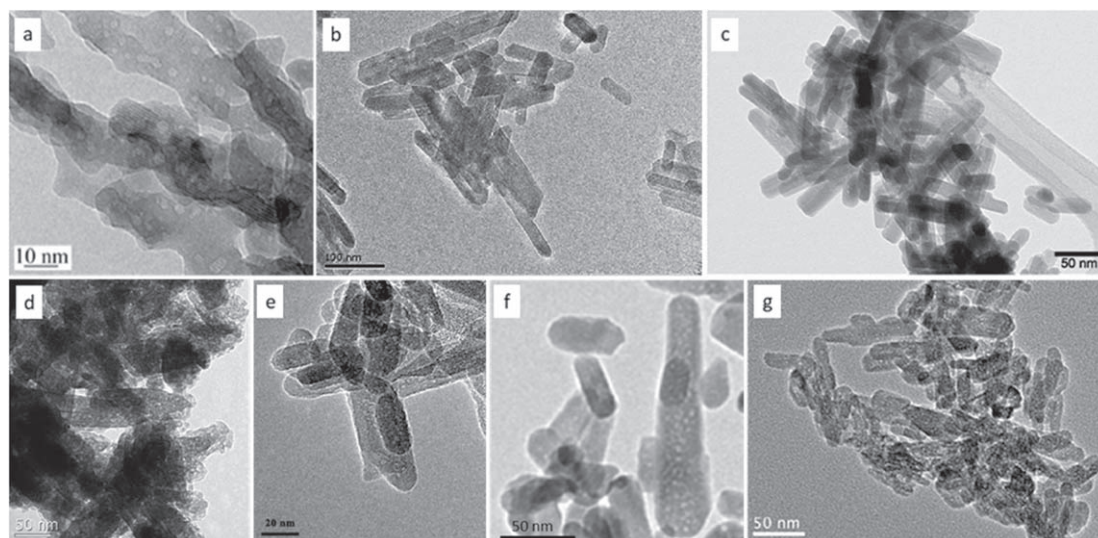


Figure 10. Mesoporous HA with physiologic-like shape obtained through different templating agents: (a)–(c) CTAB [17, 50, 51], (d)–(e) Pluronic F127 [27, 52], (f) Triton X-100 [23] and (g) Tea polyphenols [53]. All images are reproduced with permission.

regulation of mesopores features. In fact, Wang *et al* [17] highlighted that CTAB has an evident effect on the surface area, the pore volume and the pore size of HA particles. Indeed, samples produced without surfactant showed a relatively small surface area of $33 \text{ m}^2 \text{ g}^{-1}$ and no porous structure, whereas samples obtained with the addition of CTAB in a proper amount, showed higher surface area with open-ended pores ranging between 2 and 7 nm, as revealed by TEM images. More specifically, the sample with a CTAB:HA precursors molar ratio equal to 1:2 exhibited the highest surface area ($97 \text{ m}^2 \text{ g}^{-1}$) and the largest pore volume ($0.47 \text{ cm}^3 \text{ g}^{-1}$), as visible in figure 10(a). However, with the further increase of the surfactant amount, the pore volume and the surface area decreased. It is worth to mention that the pore size distributions obtained from nitrogen adsorption-desorption measurements possessed a very broad shape, with values up to several hundreds of nanometres, ascribable to the inter-particles voids.

Concerning alternative synthesis routes, Yao *et al* [54] obtained rod-like HA structures with a mean pore size of 3 nm by refluxing at 120°C for 24 h a solution with pH 12, containing $\text{K}_2\text{HPO}_4 \cdot 3\text{H}_2\text{O}$ and CaCl_2 as HA precursors and CTAB as surfactant. These nanocavities aligned in a lengthwise direction within the rods and were obtained by the removal of CTAB micelles through calcination, conducted at 550°C for 6 h.

Benzigar *et al* [55] used the same precursors and templating agent as Yao and co-workers, but they transferred the solution mixture into a Teflon autoclave and heated it in a microwave oven at 120°C for 8 h. They synthesized nano-HA with high crystallinity and highly uniform rod-like morphology with an average size of about 25 nm in width and 100 nm in length. Through the decomposition of CTAB, they

obtained samples with a bimodal pore size distribution centred at 2.5 and 3.7 nm, according to pore size distribution obtained by nitrogen adsorption-desorption analysis. In order to elucidate the role of the single treatment, they prepared another sample using only the hydrothermal treatment without microwave irradiation and they noticed the absence of mesoporous structure. Based on this observation, the authors postulated that microwave radiation favours the precursor reaction as well as their ionic interactions with the surfactant, thus promoting at the same time the formation of a highly crystalline and mesoporous structure. Kumar *et al* [51] confirmed the efficiency of this combined method to prepare mesoporous HA nanocrystals in a rapid way (figure 10(c)) and reported the synthesis of rod-like particles having pores of around 2 nm.

In general, from the analysis of the literature works, it emerges that the introduction of CTAB in a concentration above its CMC leads to the formation of pores in 2–5 nm range throughout HA particles. The best results in terms of specific surface area and pore volume values were obtained with a CTAB concentration of 0.2–0.24 M. However, conflicting results are reported in the literature regarding the function of CTAB in the HA synthesis and the full comprehension of the surfactant role as purely shape-directing agent or as mesopore generating agent in the synthesis of HA particles is still an open question. Indeed, for instance, Shiba and collaborators [16] affirmed that CTAB mainly worked as a shape controlling agent rather than a templating agent as no clear difference in terms of mesoporosity was evidenced between HA synthesized with and without the surfactant. In addition, across the related literature, no evident and remarkable differences in terms of synthesis conditions, among which the employed CTAB concentration, have been

identified among the articles reporting the two behaviours of CTAB.

Different authors also investigated the use of non-ionic surfactants, i.e. Pluronic F127 or Pluronic P123, in the production of mesoporous HA nanorods in order to overcome the limitations of ionic surfactants, such as the relatively small pore size dimension achievable with CTAB [56]. For example, Zhao *et al* [27] obtained rod-like particles with length ranging between 100 and 300 nm, diameter around 50 nm and pore sizes ranging from 2.5 to 3 nm (as visible in figure 10(d)), using Pluronic F127 at high concentration (10 wt%). They heated up to 90 °C and refluxed for 24 h a mixture containing $K_2HPO_4 \cdot 3H_2O$ and calcium D-pantothenate monohydrate as HA precursors and adjusted the pH to 12. The obtained dried precipitate was then calcined in a furnace at 550 °C for 6 h in order to remove the block co-polymer template and to obtain the mesoporous structure. More recently, Zhang and collaborators [52] synthesized mesoporous rod-shaped HA as drug carriers by means of the hydrothermal method using the same surfactant. Even in this case, they produced samples with dimensions similar to the previous ones and with pores prevalently around 3 nm (figure 10(e)), as revealed by both adsorption analysis and TEM images.

In the work of Iyyappan *et al* [23], nanoporous HA was prepared via hydrothermal treatment using Triton X-100 (figure 10(f)). More in detail, the authors obtained samples with a combination of meso- and macropores ranging between 7.4 and 55 nm. The authors attributed this broad pore size distribution to the presence of internal mesopores and of intra-particle voids deriving by the agglomeration of primary HA particles. Since the pore size distribution of samples produced without the use of the surfactant or without the hydrothermal treatment presented even broader pore size distributions, the authors affirmed that Triton X-100 has a beneficial role in reducing the agglomeration of HA particles. Moreover, they demonstrated that the total pore volume and the percentage of mesoporous volume were higher for samples prepared by the hydrothermal method than those obtained under a non-hydrothermal route, particularly in the absence of the organic modifier.

In addition to the above-reported surfactants, it is worth mentioning the class of zwitterionic surfactants, whose ionic features are determined by the pH of the medium. In particular, they exhibit cationic behaviour near or below their isoelectric point and turn to be anionic for higher pHs. In this regard, Amer *et al* [57] produced nano-structured HA using lauryl dimethylaminoacetic acid as zwitterionic surfactant under microwave irradiation conditions. They obtained rod-like structures with a uniform diameter and length of about 19 nm and 69 nm respectively. N_2 adsorption analysis revealed a surface area of $87 \text{ m}^2 \text{ g}^{-1}$ and pores with an average size of 36 nm. Since this latter value is of the same order of magnitude of the particle

dimensions, it is possible to affirm that the inter-particle porosity strongly contributed to the pore size distribution and shifted upward the average size. In order to confirm the influence of the template on the HA structural features, the authors repeated the same synthesis procedure without the use of surfactants obtaining samples with low surface area ($30 \text{ m}^2 \text{ g}^{-1}$). An inferior value of surface area ($20 \text{ m}^2 \text{ g}^{-1}$) was also achieved in the presence of the surfactant but by conventional heating. In this way, the authors demonstrated the advantage of combining microwave heating with surfactants to increase the surface area of HA particles.

Some authors investigated the effect of pH-control techniques on the characteristics of mesoporous HA. For example, Mohammad *et al* [56] found that the continuous pH adjustment throughout the mixing of the precursor solutions was very effective in favouring the production of particles with controlled textural properties. In fact, the particles synthesised by maintaining the pH at 11 by the addition of NaOH throughout the mixing process had higher surface area and more uniform pore size distribution compared to those obtained by controlling the pH only before the solution mixing. The formation of micelles is indeed inhibited by the sharp pH decrease occurring when the two solutions are mixed, due to the nature of the calcium precursor ($CaCl_2 \cdot 2H_2O$). Therefore, through the continuous control of the synthesis solution pH, the formation of micelles is favoured and larger amount of pores are consequently generated throughout the particles, with a resulting increase of the final surface area.

Recently, new attempts have been made to find novel cost-effective and sustainable sources for the preparation of such materials. For example, in 2017 Zhou *et al* [58] reported a simple and rapid strategy for the hydrothermal synthesis of mesoporous HA nanoparticles based on the use of sodium hexametaphosphate ($Na_6P_6O_{18}$) as phosphorous source and tea polyphenols as templating agents. The advantage of these reagents is that they can be completely removed by a washing step (without calcination) and are more environmentally friendly compared to traditional agents as CTAB. The resulting nanoparticles exhibited a very high surface area ($114 \text{ m}^2 \text{ g}^{-1}$) and a uniform pore size distribution (4–9 nm). Tea polyphenols, due to the high amount of hydroxyl groups can bind Ca^{2+} ions and consequently guide the arrangement of HA particles. In fact, the HA synthesised in the absence of the polyphenols showed a disordered arrangement of the inter-particle porosity deriving from the random hydrolysis of phosphate precursor ($Na_6P_6O_{18}$) in the aqueous solution. Instead, when polyphenols are present, they can act as template to guide the assembly of HA particles resulting in a more ordered inter-particle porosity. In 2018, the same group [53] reported the hydrothermal synthesis of mesoporous rod-like HA nanoparticles using vitamin C as cost-effective templating agent. The synthesized particles, visible in

Table 1. Summary and comparison of various methods in physiologic-like HA synthesis.

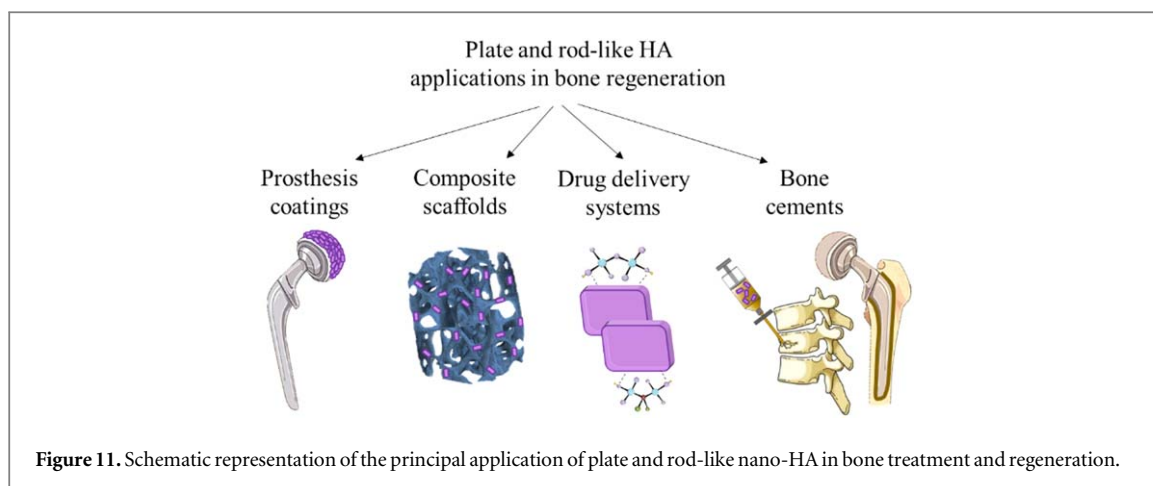
HA aspect	Shape	Type of synthesis	Surfactant	Type of surfactant	Article
Physiologic-like	Plate	Hydrothermal	Ethylamine	cationic	Nagata <i>et al</i> [28]
		Hydrothermal	STPP	anionic	Zhang <i>et al</i> [22]
		Emulsion	AOT	anionic	Sato <i>et al</i> [19]
		Microwave	CTAB	cationic	Arami <i>et al</i> [30]
	Rod	Hydrothermal	CTAB	cationic	Wang <i>et al</i> [32]
		Hydrothermal	CTAB	cationic	Wang <i>et al</i> [33]
		Hydrothermal	SDS	anionic	Yan <i>et al</i> [34]
		Hydrothermal	CTAB	cationic	
		Hydrothermal	PEG-600	non-ionic	Wang <i>et al</i> [35]
			Tween-20	non-ionic	
			Trisodium citrate	non-ionic	
		Hydrothermal	EDTA	anionic	Xin <i>et al</i> [36]
		Hydrothermal	EDTA + CTAB	anionic + cationic	Xue <i>et al</i> [38]
		Emulsion	Triton X-100 + CTAB	non-ionic + cationic	Sun <i>et al</i> [39]
		Hydrothermal combined with microemulsion	CTAB	cationic	Lin <i>et al</i> [37]
		Microwave	EDTA	anionic	Liu <i>et al</i> [40]
		Microwave	EDTA	anionic	Lak <i>et al</i> [41]
		Microwave	EDTA	anionic	Kalita <i>et al</i> [21]
		Precipitation in reflux conditions	Triton X-100	non-ionic	Iyyappan <i>et al</i> [25]
		Precipitation in reflux conditions	CTAB	cationic	Shiba <i>et al</i> [16]
		Hydrothermal	CTAB	cationic	Loo <i>et al</i> [44]
			SDS	anionic	
Mesoporous	Rod	Hydrothermal	CTAB	cationic	Li <i>et al</i> [50]
		Hydrothermal	CTAB	cationic	Wang <i>et al</i> [17]
		Precipitation in reflux conditions	CTAB	cationic	Yao <i>et al</i> [54]
		Hydrothermal combined with microwave	CTAB	cationic	Benzigar <i>et al</i> [55]
		Hydrothermal combined with microwave	CTAB	cationic	Kumar <i>et al</i> [51]
		Precipitation in reflux conditions	Pluronic F127	non-ionic	Zhao <i>et al</i> [27]
		Hydrothermal	Pluronic F127	non-ionic	Zhang <i>et al</i> [52]
		Hydrothermal	Triton X-100	non-ionic	Iyyappan <i>et al</i> [23]
		Microwave	Lauryl dimethylaminoacetic	zwitterionic	Amer <i>et al</i> [57]
		Hydrothermal	Tea polyphenols	non-ionic	Zhou <i>et al</i> [58]
		Hydrothermal	Vitamin C	non-ionic	Zhou <i>et al</i> [53]

figure 10(g), were characterized by a surface area of about $39 \text{ m}^2 \text{ g}^{-1}$ and a mean pore size of 20 nm. The authors suggested the following mechanism underlying the mesopore formation: the vitamin C molecules are partially adsorbed via their abundant –OH groups on the surface of the growing HA, hindering its further growth. Therefore, HA crystals are forced to grow exclusively on the vitamin-free surfaces and entrap the vitamin molecules inside them. Vitamin C is then removed by the hydrothermal treatment, leading to the formation of the mesopores.

The scientific studies analysed in this review are summarized in table 1, in order to enable researchers with a comprehensive overview of physiologic-like and mesoporous HA synthesis routes.

5. The use of plate and rod-like HA in bone treatment and regeneration

As previously introduced, synthetic nano-HA has found numerous applications in the biomedical field, thanks to its biocompatibility, osteoconductivity and



overall biological properties deriving from its biomimetic chemical composition and high surface area. To further enhance the properties of HA particles, their crystalline structure has been modified through the substitution of calcium, phosphate or hydroxyl groups with other ions. Depending on the type of biological response requested, different ions can be considered for the substitution. In particular, strontium, magnesium and zinc ions, which occupy calcium sites in the HA crystal lattice, are reported to increase nano-HA solubility and improve osteoblast attachment and proliferation, thus leading to a superior reactivity and osteoconductivity of the material [59, 60]. On the other hand, carbonate, silicate and fluorine ions can substitute both phosphate and hydroxyl groups, conferring to the material an improved osteoconductive potential as well as superior mechanical properties due to an increase of HA crystallinity [60].

Within the biomedical field, pure and doped nano-HAs have found their principal applications in the bone tissue engineering area thanks to their osteoconductive potential. For this reason, synthetic HA has been used as coating for metallic orthopaedic implants, filler for bone cements, drug delivery system or constituent of bone scaffolds, as schematically represented in figure 11. In this section, the main applications of nano-HA in the bone engineering area are reported, with a particular focus on the studies concerning the use of plate or rod-like particles, since they represent the main topic of this review.

The use of nano-HA as coatings on orthopaedic implants proved to be a successful solution to improve the osteointegration at the surgical site. In fact, orthopaedic implants are usually made by titanium alloys having excellent mechanical properties, but not able to stimulate a biological response in the host tissue due to their superficial oxide layer that hinders bone cell adhesion. On the contrary, the presence of a HA coating of approximately 50 μm in thickness has been associated with the stimulation of new bone growth on the implant, leading to its improved fixation [59]. The good adhesion of the HA coating on the substrate is a key factor and it is specifically required to avoid fatigue

failure or the detachment of the coating and can be obtained by a strict control of the process parameters and of the particle properties [61].

Another application of nano-HA is related to its use as osteoconductive filler in bone cements for the treatment of fractures or the fixation of orthopaedic prosthesis. Since the cement is usually constituted by an inert material (e.g. poly methyl methacrylate), the addition of the nano-HA phase can lead to an improvement of its biological behaviour [62]. In fact, thanks to the osteoconductive potential of nano-HA, a stronger bond can be formed between the cement and the bone tissue leading to a better integration of the implant. Similarly, cements able to promote new bone formation are fundamental in the case of osteoporotic fracture fixation, where the risk of loosening and failure of the implant is high due to the reduced healing potential of osteoporotic patients [63]. In the frame of the studies reporting the use of rod-like nano-HA as osteoconductive phase in bone cements, it is worth to mention the work conducted by Che and co-workers [62]. In particular, they observed that the introduction of rod-like nano-HA particles, synthesised using PEG2000 as templating agent, in a PMMA-based cement increased the mineralisation degree of the cement surface while enhancing bone progenitor cell proliferation compared to the pure PMMA cement. Similarly, Li and co-workers produced rod-like nano-HA particles using PEG400 as templating agent and, subsequently, introduced them in an injectable polyurethane-based cement obtaining an improvement of its mechanical and bioactive properties [64].

Nano-HA is also particularly attractive as drug carrier due to its solubility in the biological fluids and its capacity to penetrate the cell membrane [65]. Furthermore, thanks to its chemical composition and structure, nano-HA can successfully interact with several compounds. A remarkable interaction has been observed with bisphosphonates, specific drugs used for the anti-resorptive therapy of osteoporosis, thanks to their strong affinity to calcium ions. This interaction was confirmed by Boanini *et al* that synthesised pure and Sr-substituted nano-HA particles with

rod-like morphology in the presence of disodium zoledronate tetrahydrate, observing a high loading rate [66, 67]. Moreover, the combination of nano-HA and zoledronate led to an improved biological response, increasing osteoblast proliferation and differentiation, while decreasing osteoclast survival. These effects were further enhanced in presence of strontium-doped nano-particles, demonstrating their potential in anti-osteoporotic treatments.

The improved biological effect arising from the combination of doped-HA and bisphosphonates was also observed by Khajuria and collaborators [68]. In particular, they investigated the incorporation of risendronate in Zn-doped HA nanoparticles with the aim of creating a suitable vector for its non-oral administration. The authors tested the combined system on ovariectomised rats observing a superior recover of the osteoporosis-induced bone damage thanks to the beneficial action of zinc in enhancing bone formation and mineralisation.

In recent years, innovative systems combining nano-HA and other inorganic nanoparticles having peculiar physical properties have been investigated by several research groups to explore novel applications in the bone regeneration field. For example, Tran and Webster proposed an alternative treatment for osteoporosis combining magnetite nanoparticles and rod-like nano-HA synthesised through a hydrothermal method. The combined system proved to stimulate the expression of several differentiation markers in osteoblasts (ALP activity, collagen synthesis and calcium deposition), highlighting its high osteogenic potential. Furthermore, thanks to the presence of magnetite nanoparticles, this stimulating action can be directed at specific sites (e.g. the osteoporotic fracture site) through to the use of a magnetic field [69]. Khajuria and collaborators, instead, conjugated nitrogen-doped carbon dots with HA nanoparticles through a hydrothermal co-precipitation synthesis [70]. The system proved its bone regeneration potential both *in vitro* promoting osteoblast proliferation, differentiation and mineralisation and *in vivo* enhancing the bone growth and the mineral density of a zebrafish jawbone model. Furthermore, thanks to the luminescence shown by the carbon dots, the system can be exploited for theragnostic applications.

Lastly, another promising and reported application of plate-like and rod-like HA nanoparticles in the bone field is their use as reinforcing phase in composite scaffolds for bone tissue regeneration. In fact, their addition in a polymeric matrix can improve the scaffold mechanical properties and stimulate the growth of new bone thanks to their biomimetic morphology and composition [59]. In order to achieve the desired improvement of mechanical and biological performances, HA particles need to be homogeneously dispersed in the matrix avoiding the formation of aggregates. Different types of polymers have been used

as matrix for scaffold preparation, both natural and synthetic. For example, Sartuqui and co-workers suspended rod-like HA, synthesised by means of the hydrothermal treatment in presence of CTAB as templating agent, in a gelatine-based matrix [71]. The gelatine suspension was successively crosslinked with tannic acid and freeze-dried. The presence of HA particles led to an improvement of scaffold mechanical properties and of its mineralisation degree when immersed in SBF, confirming its osteoconductive potential. Similar results were observed by Zandi and co-workers, who tested the mechanical and biological behaviour of an HA-gelatine freeze-dried scaffold [72]. The composite scaffold promoted an increased bone cell adhesion and proliferation compared to the pure gelatine scaffold, thanks to the beneficial action of HA particles in creating a more biomimetic material. Collagen is another natural polymer frequently used as matrix in bone scaffold fabrication thanks to its highly biomimetic structure mimicking the extracellular matrix. Zheng and co-workers produced a collagen-HA scaffold, synthesising rod-like HA particles through the hydrothermal method while exploiting the genipin crosslinking and the freeze-drying technique to produce the composite scaffold. Due to its high structural and compositional biomimicry, the scaffold induced a superior bone cell adhesion, proliferation and differentiation rate [73].

Synthetic polymers have been largely adopted for bone scaffold fabrication since they enable a higher control over the final properties of the scaffold, such as degradation kinetics and mechanical properties. On the contrary, they proved less biocompatibility and lack of cell-recognize sites. The design of composite scaffolds through the addition of HA particles can increase the osteoconductive potential of these polymers, leading to an increase of bone cell adhesion and proliferation. The beneficial effects linked to the addition of HA in the material formulation were observed by Huang and co-workers who developed a composite scaffold constituted by poly-2-hydroxyethylmethacrylate, polycaprolactone and rod-like HA particles [74]. Similarly, Nejati and co-workers fabricated a poly(L-lactide acid)-based scaffold reinforced by rod-like HA particles, observing an increase of scaffold mechanical properties compared to the pure polymeric scaffold [75]. Also in this case, the addition of HA particles led to a significant increase of bone cell adhesion and proliferation, highlighting the high osteoconductive potential of this material.

6. Conclusions

Considering the promising results observed in bone tissue regeneration field thanks to the use of nano-HA, the research community have focused its attention on the enhancement of HA synthesis methods in order to produce nanoparticles with improved features.

In this review, the various techniques used to synthesize physiologic-like shaped and mesoporous nano-HA were described with a comprehensive and critical review of the literature data. A prevalence of non-conventional methods, i.e. hydrothermal, emulsion and microwave irradiation, combined with the use of different surfactants is mostly proposed for the synthesis of nano-sized HA with peculiar shape (i.e. rod-like, plate-like) and structural features (i.e. high surface area, accessible mesopores).

In particular, the hydrothermal approach allows obtaining pure and highly crystalline HA in the form of rods and plates, although it involves high temperatures and is a time-consuming process. On the other hand, microwave irradiation leads to the formation of particles with high purity and narrow particle size in a very fast way. In the end, microemulsion might be an effective strategy to synthesize and regulate more accurately the size and the shape of HA crystals. Furthermore, the combination of these methods can overcome the drawbacks and combine the advantages of each single technique. The use of surfactants in the above-mentioned synthesis techniques allows a better control of the HA morphology, since these molecular agents are able to direct the growth of HA particles toward a specific direction thanks to the occurrence of selective interactions with HA precursors. Among the templating agents reported in the literature, the CTAB turned out to be the most widely used, although more recently different authors adopted natural and non-toxic templating agents like vitamin C and tea polyphenols for the synthesis of HA through a more environmentally friendly approach.

Focusing on the plate-like HA crystals, a strict control over the synthesis parameters is generally required to achieve this morphology. In case of hydrothermal synthesis, a key role is played by the surfactant concentration required to direct the growth of HA particles toward the plate-like morphology. High supersaturation concentration of HA precursors and high microwave power are reported to be beneficial for the synthesis of plate-like HA through the microemulsion process and the microwave method, respectively.

Rod-like HA particles are generally obtained through the hydrothermal method, in the presence of alkaline conditions, autoclaving temperatures above 100 °C and durations of around 20 h. Higher hydrothermal temperatures and longer treatments lead to the production of HA with high crystallinity and large crystal size. Rod-like particles are also successfully synthesised through high-power microwave irradiation and the precipitation method under refluxing conditions thanks to the creation of a controlled and stable environment.

The same techniques in combination with surfactants at specific concentrations are also employed for the synthesis of mesoporous HA. The generated intra-particle mesopores have dimensions comprised between 2 and 10 nm, randomly distributed throughout the HA

particles. In most cases along with this intra-particle porosity, the presence of pores with a dimension of several tens of nanometres is usually reported in the literature works due to inter-particle voids resulting from the agglomeration of primary nano-sized HA crystals.

In conclusion, due to the high heterogeneity of methods and data reported in the literature, this review aims to constitute a precious background and a useful tool for those researchers that face for the first time the challenges related to the synthesis of physiologic-like or mesoporous HA in view of a biomedical application.

7. Future perspectives

The majority of articles concerning the synthesis of rod or plate-like HA concentrate exclusively on its morphological/structural characterisation, while only few works examined also its behaviour in term of cytocompatibility, osteoconductivity and stimulation of additional biological responses. Therefore, further studies are needed to evaluate the overall biological behaviour of the synthesized HA and the effective biomimicry of the physiological nanostructures, in order to produce particles suitable for bone regeneration applications.

In addition, the true control of HA particles in the term of size and shape is still an open issue, as revealed by the heterogeneous dimensions and structural features reported in the literature. With the aim to improve the control of HA textural properties, the combination of different synthesis methods, such as the hydrothermal route with the microemulsion technique, constitutes a promising strategy to be further explored.

In addition, the currently available synthesis methods allow to achieve mesopores not uniform in size and not homogeneously distributed across the HA particles. A well-organized arrangement of the porosity would produce a further increase of the exposed surface area and, consequently, an increase of HA biological reactivity. Furthermore, narrow-size and organized mesoporosity would lead to enhanced drug loading capacity and to higher reproducibility in the loading and release behaviour of HA particles, making them particularly suitable for biomedical applications. To address this issue and to cope with the need of resource-efficient and green synthesis methods, new natural organic molecules (i.e. polyphenols, vitamins) are gaining increasing interest as templating agents, due to their effective role in the mesoporosity regulation.

In the end, the scalability of the synthesis process is a key issue to consider in the selection of the most appropriate route for the HA production for biomedical applications. Nevertheless, there is a lack of works investigating the scalability of the most common synthesis methods, therefore evidencing the necessity of future studies in this perspective.

Acknowledgments

This project has received funding from the European Research Council (ERC) under the European Union's Horizon 2020 research and innovation programme (grant agreement No 681798-BOOST) (www.ercprojectboost.eu).

ORCID iDs

Sonia Fiorilli  <https://orcid.org/0000-0002-2986-0528>

Chiara Vitale-Browarone  <https://orcid.org/0000-0003-2413-5594>

References

- [1] Bala Y and Seeman E 2015 Bone's material constituents and their contribution to bone strength in health, disease, and treatment *Calcif. Tissue Int.* **97** 308–26
- [2] Rho J Y, Kuhn-Spearing L and Zioupos P 1998 Mechanical properties and the hierarchical structure of bone *Med. Eng. Phys.* **20** 92–102
- [3] Fratzl P, Gupta H S, Paschalis E P and Roschger P 2004 Structure and mechanical quality of the collagen-mineral nano-composite in bone *J. Mater. Chem.* **14** 2115–23
- [4] Mohammad N F, Othman R and Yee-Yeoh F 2014 Nanoporous hydroxyapatite preparation methods for drug delivery applications *Rev. Adv. Mater. Sci.* **38** 138–47
- [5] Shavandi A, Bekhit A E-D A, Sun Z F and Ali A 2015 A review of synthesis methods, properties and use of hydroxyapatite as a substitute of bone *J. Biomimetics, Biomater. Biomed. Eng.* **25** 98–117
- [6] Bala Y, Farlay D and Boivin G 2013 Bone mineralization: from tissue to crystal in normal and pathological contexts *Osteoporos. Int.* **24** 2153–66
- [7] Dorozhkin S V 2010 Nanosized and nanocrystalline calcium orthophosphates *Acta Biomater.* **6** 715–34
- [8] Sadat-Shojai M, Khorasani M T, Dinpanah-Khoshdargi E and Jamshidi A 2013 Synthesis methods for nanosized hydroxyapatite with diverse structures *Acta Biomater.* **9** 7591–621
- [9] Lin K, Wu C and Chang J 2014 Advances in synthesis of calcium phosphate crystals with controlled size and shape *Acta Biomater.* **10** 4071–102
- [10] Pramanik N, Tarafdar A and Pramanik P 2007 Capping agent-assisted synthesis of nanosized hydroxyapatite: comparative studies of their physicochemical properties *J. Mater. Process. Technol.* **184** 131–8
- [11] Uskoković V and Uskoković D P 2011 Nanosized hydroxyapatite and other calcium phosphates: chemistry of formation and application as drug and gene delivery agents *J. Biomed. Mater. Res. B* **96B** 152–91
- [12] Chen F, Zhu Y, Wu J, Huang P and Cui D 2012 Nanostructured calcium phosphates: preparation and their application in biomedicine *Nano Biomed. Eng.* **4** 41–9
- [13] Dorozhkin S V and Epple M 2002 Biological and medical significance of calcium phosphates *Angew. Chemie Int. Ed.* **41** 3130–46
- [14] Zhou H and Lee J 2011 Nanoscale hydroxyapatite particles for bone tissue engineering *Acta Biomater.* **7** 2769–81
- [15] Haider A, Haider S, Han S S and Kang I-K 2017 Recent advances in the synthesis, functionalization and biomedical applications of hydroxyapatite: a review *RSC Adv.* **7** 7442–58
- [16] Shiba K, Motozuka S, Yamaguchi T, Ogawa N, Otsuka Y, Ohnuma K, Kataoka T and Tagaya M 2016 Effect of cationic surfactant micelles on hydroxyapatite nanocrystal formation: an investigation into the inorganic-organic interfacial interactions *Cryst. Growth Des.* **16** 1463–71
- [17] Wang J, Huang S P, Hu K, Zhou K C and Sun H 2015 Effect of cetyltrimethylammonium bromide on morphology and porous structure of mesoporous hydroxyapatite *Trans. Nonferrous Met. Soc. China (English Ed.)* **25** 483–9
- [18] Kolodziejczak-Radzimska A, Samuel M, Paukszta D, Piasecki A and Jesionowski T 2014 Synthesis of hydroxyapatite in the presence of anionic surfactant *Physicochem. Probl. Miner. Process.* **50** 225–36
- [19] Sato K, Hotta Y, Nagaoka T, Yasuoka M and Watari K 2006 Agglomeration control of hydroxyapatite nano-crystals grown in phase-separated microenvironments *J. Mater. Sci.* **41** 5424–8
- [20] Sarda S, Heughebaert M and Lebugle A 1999 Influence of the type of surfactant on the formation of calcium phosphate in organized molecular systems *Chem. Mater.* **11** 2722–7
- [21] Kalita S J and Verma S 2010 Nanocrystalline hydroxyapatite bioceramic using microwave radiation: synthesis and characterization *Mater. Sci. Eng. C* **30** 295–303
- [22] Zhang H, Zhou K, Li Z-Y and Huang S 2009 Plate-like hydroxyapatite nanoparticles synthesized by the hydrothermal method *J. Phys. Chem. Solids* **70** 243–8
- [23] Iyyappan E, Wilson P, Sheela K and Ramya R 2016 Role of triton X-100 and hydrothermal treatment on the morphological features of nanoporous hydroxyapatite nanorods *Mater. Sci. Eng. C* **63** 554–62
- [24] Zhang J, Jiang D, Zhang J, Lin Q and Huang Z 2010 Synthesis of organized hydroxyapatite (HA) using triton X-100 *Ceram. Int.* **36** 2441–7
- [25] Iyyappan E and Wilson P 2013 Synthesis of nanoscale hydroxyapatite particles using triton X-100 as an organic modifier *Ceram. Int.* **39** 771–7
- [26] Azzaoui K, Lamhamdi A, Mejdoubi E, Berrabah M, Elidrissi A, Hammouti B, Zaoui S and Yahyaoui R 2013 Synthesis of nanostructured hydroxyapatite in presence of polyethylene glycol 1000 *J. Chem. Pharm. Res.* **5** 1209–16
- [27] Zhao Y F and Ma J 2005 Triblock co-polymer templating synthesis of mesostructured hydroxyapatite *Microporous Mesoporous Mater.* **87** 110–7
- [28] Nagata F, Toriyama M, Teraoka K and Yokogawa Y 2001 Influence of ethylamine on the crystal growth of hydroxyapatite crystals *Chem. Lett.* **30** 780–1
- [29] Siddharthan A, Seshadri S K and Kumar T S S 2006 Influence of microwave power on nanosized hydroxyapatite particles *Scr. Mater.* **55** 175–8
- [30] Arami H, Mohajerani M, Mazloumi M, Khalifehzadeh R, Lak A and Sadrnezhad S K 2009 Rapid formation of hydroxyapatite nanostrips via microwave irradiation *J. Alloys Compd.* **469** 391–4
- [31] Saha S K, Banerjee A, Banerjee S and Bose S 2009 Synthesis of nanocrystalline hydroxyapatite using surfactant template systems: role of templates in controlling morphology *Mater. Sci. Eng. C* **29** 2294–301
- [32] Wang Y, Chen J, Wei K, Zhang S and Wang X 2006 Surfactant-assisted synthesis of hydroxyapatite particles *Mater. Lett.* **60** 3227–31
- [33] Wang Y, Zhang S, Wei K, Zhao N, Chen J and Wang X 2006 Hydrothermal synthesis of hydroxyapatite nanopowders using cationic surfactant as a template *Mater. Lett.* **60** 1484–7
- [34] Yan L, Li Y, Deng Z X, Zhuang J and Sun X 2001 Surfactant-assisted hydrothermal synthesis of hydroxyapatite nanorods *Int. J. Inorg. Mater.* **3** 633–7
- [35] Wang A, Liu D, Yin H, Wu H, Wada Y, Ren M, Jiang T, Cheng X and Xu Y 2007 Size-controlled synthesis of hydroxyapatite nanorods by chemical precipitation in the presence of organic modifiers *Mater. Sci. Eng. C* **27** 865–9
- [36] Xin R, Ren F and Leng Y 2010 Synthesis and characterization of nano-crystalline calcium phosphates with EDTA-assisted hydrothermal method *Mater. Des.* **31** 1691–4
- [37] Lin K, Chang J, Cheng R and Ruan M 2007 Hydrothermal microemulsion synthesis of stoichiometric single crystal hydroxyapatite nanorods with mono-dispersion and narrow-size distribution *Mater. Lett.* **61** 1683–7
- [38] Xue C, Chen Y, Huang Y and Zhu P 2015 Hydrothermal synthesis and biocompatibility study of highly crystalline carbonated hydroxyapatite nanorods *Nanoscale Res. Lett.* **10** 1–6

- [39] Sun Y, Guo G, Wang Z and Guo H 2006 Synthesis of single-crystal HAP nanorods *Ceram. Int.* **32** 951–4
- [40] Liu J, Li K, Wang H, Zhu M and Yan H 2004 Rapid formation of hydroxyapatite nanostructures by microwave irradiation *Chem. Phys. Lett.* **396** 429–32
- [41] Lak A, Mazloumi M, Mohajerani M S, Zanganeh S, Shayegh M R, Kajbafvala A, Arami H and Sadrnezhaad S K 2008 Rapid formation of mono-dispersed hydroxyapatite nanorods with narrow-size distribution via microwave irradiation *J. Am. Ceram. Soc.* **91** 3580–4
- [42] Wang P, Li C, Gong H, Jiang X, Wang H and Li K 2010 Effects of synthesis conditions on the morphology of hydroxyapatite nanoparticles produced by wet chemical process *Powder Technol.* **203** 315–21
- [43] Khalid M, Mujahid M, Amin S, Rawat R S, Nusair A and Deen G R 2013 Effect of surfactant and heat treatment on morphology, surface area and crystallinity in hydroxyapatite nanocrystals *Ceram. Int.* **39** 39–50
- [44] Loo S C J, Siew Y E, Ho S, Boey F Y C and Ma J 2008 Synthesis and hydrothermal treatment of nanostructured hydroxyapatite of controllable sizes *J. Mater. Sci., Mater. Med.* **19** 1389–97
- [45] Bilton M 2012 Comparison of hydrothermal and sol-gel synthesis of nano-particulate hydroxyapatite by characterisation at the bulk and particle level open *J. Inorg. Non-Metallic Mater.* **02** 1–10
- [46] Sing K S W, Everett D H, Haul R A W, Moscou L, Pierotti R A, Rouquerol J and Siemieniowska T 1985 Reporting physisorption data for gas/solid systems with special reference to the determination of surface area and porosity *Pure Appl. Chem.* **57** 603–19
- [47] Moritz M and Geszke-Moritz M 2015 Mesoporous materials as multifunctional tools in biosciences: principles and applications *Mater. Sci. Eng. C* **49** 114–51
- [48] Patel V, Dharaiya N, Ray D, Aswal V K and Bahadur P 2014 PH controlled size/shape in CTAB micelles with solubilized polar additives: a viscometry, scattering and spectral evaluation *Colloids Surfaces A* **455** 67–75
- [49] Attwood D, Collett J H and Tait C J 1985 The micellar properties of the poly(oxyethylene) - poly(oxypropylene) copolymer pluronic F127 in water and electrolyte solution *Int. J. Pharm.* **26** 25–33
- [50] Li Y, Tjandra W and Tam K C 2008 Synthesis and characterization of nanoporous hydroxyapatite using cationic surfactants as templates *Mater. Res. Bull.* **43** 2318–26
- [51] Kumar G S, Karunakaran G, Girija E K, Kolesnikov E, Van M N, Gorshenkov M V and Kuznetsov D 2018 Size and morphology-controlled synthesis of mesoporous hydroxyapatite nanocrystals by microwave-assisted hydrothermal method *Ceram. Int.* **44** 11257–64
- [52] Zhang W, Chai Y, Xu X, Wang Y and Cao N 2014 Rod-shaped hydroxyapatite with mesoporous structure as drug carriers for proteins *Appl. Surf. Sci.* **322** 71–7
- [53] Zhou H, Yang Y, Yang M, Wang W and Bi Y 2018 Synthesis of mesoporous hydroxyapatite via a vitamin C templating hydrothermal route *Mater. Lett.* **218** 52–5
- [54] Yao J, Tjandra W, Chen K Y Z, Tam K C, Ma J and Soh B 2003 Hydroxyapatite nanostructure material derived using cationic surfactant as a template *J. Mater. Chem.* **13** 3053–7
- [55] Benzigar M R, Mane G P, Talapaneni S N, Varghese S, Anand C, Aldeyab S S, Balasubramanian V V and Vinu A 2012 Microwave-assisted synthesis of highly crystalline mesoporous hydroxyapatite with a rod-shaped morphology *Chem. Lett.* **41** 458–60
- [56] Mohammad N F, Othman R and Yeoh F Y 2014 Controlling the pore characteristics of mesoporous apatite materials: hydroxyapatite and carbonate apatite *Ceram. Int.* **41** 10624–33
- [57] Amer W, Abdelouahdi K, Ramanarivo H R, Zahouilly M, Fihri A, Coppel Y, Varma R S and Solhy A 2013 Synthesis of mesoporous nano-hydroxyapatite by using zwitterions surfactant *Mater. Lett.* **107** 189–93
- [58] Zhou H, Yang M, Hou S and Deng L 2017 Mesoporous hydroxyapatite nanoparticles hydrothermally synthesized in aqueous solution with hexametaphosphate and tea polyphenols *Mater. Sci. Eng. C* **71** 439–45
- [59] Gomes D S, Santos A M C, Neves G A and Menezes R R 2019 A brief review on hydroxyapatite production and use in biomedicine *Ceramica* **65** 282–302
- [60] Ratnayake J T B, Mucalo M and Dias G J 2017 Substituted hydroxyapatites for bone regeneration: a review of current trends *J. Biomed. Mater. Res. B* **105** 1285–99
- [61] Szcześ A, Hołysz L and Chibowski E 2017 Synthesis of hydroxyapatite for biomedical applications *Adv. Colloid Interface Sci.* **249** 321–30
- [62] Che Y, Min S, Wang M, Rao M and Quan C 2019 Biological activity of hydroxyapatite/poly(methylmethacrylate) bone cement with different surface morphologies and modifications for induced osteogenesis *J. Appl. Polym. Sci.* **136** 48188
- [63] Sterling J A and Guelcher S A 2014 Biomaterial scaffolds for treating osteoporotic bone *Curr. Osteoporos. Rep.* **12** 48–54
- [64] Li K, Zuo Y, Zou Q, Lin L, Wang L, Yang B, Hu F, Li J, Li Y and Li J 2016 Synthesis and characterization of injectable nano-hydroxyapatite/polyurethane composite cement effective formulations for management of osteoporosis *J. Nanosci. Nanotechnol.* **16** 12407–17
- [65] Fox K, Tran P A and Tran N 2012 Recent advances in research applications of nanophase hydroxyapatite *ChemPhysChem* **13** 2495–506
- [66] Boanini E, Torricelli P, Gazzano M, Fini M and Bigi A 2012 The effect of zoledronate-hydroxyapatite nanocomposites on osteoclasts and osteoblast-like cells *in vitro Biomaterials* **33** 722–30
- [67] Boanini E, Torricelli P, Gazzano M, Della Bella E, Fini M and Bigi A 2014 Combined effect of strontium and zoledronate on hydroxyapatite structure and bone cell responses *Biomaterials* **35** 5619–26
- [68] Khajuria D K, Disha C, Vasireddi R, Razdan R and Mahapatra D R 2016 Risedronate/zinc-hydroxyapatite based nanomedicine for osteoporosis *Mater. Sci. Eng. C* **63** 78–87
- [69] Tran N and Webster T J 2011 Increased osteoblast functions in the presence of hydroxyapatite-coated iron oxide nanoparticles *Acta Biomater.* **7** 1298–306
- [70] Khajuria D K, Kumar V B, Gigi D, Gedanken A and Karasik D 2018 Accelerated bone regeneration by nitrogen-doped carbon dots functionalized with hydroxyapatite nanoparticles *ACS Appl. Mater. Interfaces* **10** 19373–85
- [71] Sartuqui J, Gravina A N, Rial R, Benedini L A, Yahia L, Ruso J M and Messina P V 2016 Biomimetic fiber mesh scaffolds based on gelatin and hydroxyapatite nano-rods: designing intrinsic skills to attain bone repair abilities *Colloids Surfaces B* **145** 382–91
- [72] Zandi M, Mirzadeh H, Mayer C, Urch H, Eslaminejad M B, Bagheri F and Mivehchi H 2010 Biocompatibility evaluation of nano-rod hydroxyapatite/gelatin coated with nano-HAp as a novel scaffold using mesenchymal stem cells *J. Biomed. Mater. Res. A* **92** 1244–55
- [73] Zheng X, Hui J, Li H, Zhu C, Hua X, Ma H and Fan D 2017 Fabrication of novel biodegradable porous bone scaffolds based on amphiphilic hydroxyapatite nanorods *Mater. Sci. Eng. C* **75** 699–705
- [74] Huang J, Lin Y W, Fu X W, Best S M, Brooks R A, Rushton N and Bonfield W 2007 Development of nano-sized hydroxyapatite reinforced composites for tissue engineering scaffolds *J. Mater. Sci., Mater. Med.* **18** 2151–7
- [75] Nejati E, Mirzadeh H and Zandi M 2008 Synthesis and characterization of nano-hydroxyapatite rods/poly(L-lactide acid) composite scaffolds for bone tissue engineering *Composite A* **39** 1589–96